Nature of the 0_3^+ state in ^{152}Sm from picosecond-lifetime measurement: "Correspondence" interpretation of the 0^+ bands in heavy Sm and Gd

H. Mach, M. Hellström, B. Fogelberg, D. Jerrestam, and L. Spanier
Department of Neutron Research, University of Uppsala, S-61182 Nyköping, Sweden
(Received 10 February 1992)

A revised γ-decay scheme has been deduced for the low-spin decay of ^{152}Pm$\rightarrow^{152}$Sm and a half-life of 15(6) ps has been measured for the 0_3^+ state in ^{152}Sm. The $B(E2)$ and $\rho^2(E0)$ rates for the 0_3^+ band (previously interpreted as the shape-coexisting *spherical* band) are well reproduced by the pairing-plus-quadrupole calculations which show no shape-coexisting minima. The 0^+ systematics for heavy Sm and Gd is reexamined. Contrary to the shape-coexistence interpretation, all 0^+ band sequences evolve rapidly towards deformation: e.g., the *spherical* band still spherical for $N\leq 90$ becomes deformed for $N\geq 92$. Properties of the low-lying bands could be understood from the *correspondence* interpretation as evolving from quadrupole phonon multiplets. It is suggested that the β' band (0_3^+) represents a new mode of excitation in par with β and γ modes.

PACS number(s): 23.20.Lv, 21.10.Tg, 27.70.+q, 21.60.Ev

I. INTRODUCTION

The *abrupt* transition from spherical to deformed shapes in the heavy samarium region has become a crucial testing ground for various models including the geometrical model [1], the pairing-plus-quadrupole (PPQ) model [2–7], the boson expansion theory [8–10], the interacting boson approximation (IBA) [11], IBA incorporating shape coexistence features [12], and lately the α-clustering model [13]. These models although intrinsically different reproduce quite well the abruptness of the shape transition and numerous properties of the ground state (g.s.), β, and γ bands. The challenge to nuclear models is still provided by the higher-lying states — like the negative parity bands (and the issue of mixing of dipole, quadrupole, and octupole modes of excitation) or the second excited 0^+ bands interpreted as *shape-coexisting* [12] or m bands [2–4].

In the *shape-coexistence* picture two different structures, spherical and deformed, coexist in a nucleus. In the spherical ^{150}Sm the 0_3^+ band is deformed while in the deformed ^{152}Sm it is spherical. The "intruder" character of the 0_3^+ bands provides a natural explanation for the unusual transition strengths in the (p,t) and (t,p) reactions [14–19], the band-mixing anomalies [20–24], and the difficulties of certain models (like IBA) to account for the 0_3^+ bands [12]. The latter problem may be related to the severely truncated model space for the phenomenological models [25].

On the other hand, the microscopic PPQ calculations [2–4] account quite well for the experimental features and predict a new type of 0^+ bands (m bands) characterized by strongly mixed configurations and by a deformation similar to that of the g.s. and β bands. If these bands correspond to the 0_3^+ bands in ^{150,152}Sm, as suggested by Kumar [3], then the PPQ calculations would contradict the shape-coexistence interpretation. Yet, not enough data have been available on the 0_3^+ bands to identify them as the m bands. The band identification is further complicated by the excitation energies which are predicted well above the observed values. There is also a possibility that the *intruder* and the m bands coexist in ^{150,152}Sm, or that neither of those predictions are correct.

It is the purpose of this study to measure the lifetime and branching ratios for the 0_3^+ state in ^{152}Sm and to compare the observed transition rates to the PPQ predictions. As these transition rates were found to be in good agreement, the shape coexistence interpretation of the Sm region was put into question. Serious problems with the shape-coexistence interpretation were also found [26–28] in recent studies of the cadmium nuclei which represent another classical region of shape coexistence. Consequently, the scope of this paper was extended g.s. include (see below) the *correspondence* interpretation of the transitional Sm and Gd nuclei.

From the correspondence relations for levels in the transitional regions, one can follow [29–33] the evolution of the quadrupole vibrational multiplets (spherical nuclei) into the levels of the g.s., β, and γ bands in the deformed nuclei as schematically shown in Fig. 1. Important here is the suggestion by Sakai [30, 31] (see also Refs. [3, 33]) that bandheads of the β' bands, i.e., the 0_3^+ states, evolve from the three-phonon vibrational states. So far this suggestion has not been explicitly and rigorously tested. Besides tabulating energies of various bands [32] one has to follow specific properties of the 0^+ bands to check for band crossings and existence of other (intruder) bands at low excitation energy. The influence of γ softness on such systematics (it lowers the three-phonon 0^+ state below the two-phonon 0^+ state) has been predicted by Gneuss, Mosel, and Greiner [34] and partially tested by Meyer and co-workers [35, 36].

Recently Fahlander *et al.* [26] measured, by means of heavy-ion Coulomb excitations, an almost complete set of reduced $E2$ matrix elements for the lowest-lying positive-parity states in ^{114}Cd. Perhaps unintended by

 ©1992 The American Physical Society

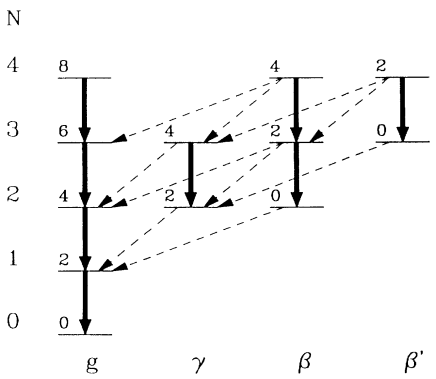

FIG. 1. The correspondence relation [30, 31] between the quadrupole vibrational multiplets and the ground state, β, γ, and β' bands in the rotational nuclei. Only selected levels are indicated, marked by the level spin (above the level bar) and by the phonon number N (in the leftmost column). Broken arrows indicate transitions which $B(E2)$ rates are high in the vibrational limit (ΔN=1) but low in the rotational one (*transitional* pattern). Solid arrows indicate transitions which $B(E2)$ rates are high in both limits (*fast* pattern). Other transitions (not shown) would follow the *slow* patterns.

the authors, this seminal work can be seen as the first rigorous comparison of the *correspondence* and the *shape-coexistence* interpretations of ^{114}Cd as the data were compared with predictions by the harmonic vibrator model and various shape-coexistence models. The data favor a vibrational-like structure involving levels up to the four-quadrupole phonon multiplet. (The 0_3^+ state, otherwise interpreted [37] as a complex intruder structure, found a simple interpretation as the three-phonon vibrational state.) In particular, strongly hindered $B(E2; 0_3^+ \rightarrow 2_1^+)$ and $B(E2; 2_3^+ \rightarrow 2_1^+)$ rates, which are difficult to account for in the shape-coexistence models (where strong configuration mixing is required), are simply interpreted as forbidden three-phonon to one-phonon transitions.

The correspondence and shape-coexistence interpretations are best tested in the transitional Sm-Gd nuclei. By adding a few neutron pairs, the transition rate pattern for the quasi-β, quasi-γ, and the most critical here, the quasi-β' bands should switch from that characteristic of a harmonic vibrator (at N=86–88) to that of a rigid rotor (at N=94–96). Consequently, in the second part of our study the energy and transition rate systematics for the 0^+ bands in heavy Sm and Gd are examined with the aim to compare, perhaps in the first study of this type, the correspondence and shape-coexistence interpretations of the low-lying bands including the crucial 0_3^+ bands.

II. EXPERIMENTAL DETAILS

Measurements of $\gamma\gamma$, fast timing $\beta\gamma\gamma$ coincidences, and γ singles were performed at the fission-product mass separator OSIRIS [38, 39] at Studsvik. The ion source was operated in the electron impact (plasma) ionization mode at a temperature of 2500 °C. The mass separated A=152 beam contained activities of ^{152}Pr, ^{152}Nd, and ^{152}Pm, including the three known Pm isomers. No significant contamination from molecular sidebands was observed. Levels in ^{152}Sm were populated in the β^- decay of ^{152}Pm. Section II A describes the γ-ray measurements, while section II B provides a brief account of the fast timing $\beta\gamma\gamma(t)$ method [40–43] used in the lifetime measurements, including details relevant to the present measurement. This recently developed method allows for the first time to measure systematically lifetimes down to the few-picosecond range for the states populated in the β^- decays. (The lifetimes of the 2_1^+ states in ^{152}Nd and ^{152}Sm that were measured in the same experiment have already been published [44].)

A. γ measurements

For the $\gamma\gamma$ measurements a multidetector system was used consisting of five detectors [one 80% HPGe detector, three 15–20 % Ge detectors and one planar low energy photon (LEP) detector] positioned in a plane around the direct-beam collection point. The beam was collected onto a movable Al-coated Mylar tape in a cycle of 10 s. The old sample was removed before starting a new cycle. About 4×10^7 $\gamma\gamma$ coincidences were recorded and sorted off line. In the off-line analysis the $\gamma\gamma$ coincidences were gain corrected and sorted into a two-dimensional matrix. Background subtracted coincident spectra were obtained for all observed γ rays.

Two multispectrum scaling measurements were performed: one with a 80% HPGe detector for the high-energy γ rays and one with a LEP detector for the low-energy transitions. The measurement cycle comprised of 6 s of beam collection followed by eight consecutive spectral measurements of 1.0 s duration each before removal of the old sample. This measurement allowed identification of any short-lived activities from the little-known ^{152}Ce→^{152}Pr ($T_{1/2}$=1.4 s) [45] and ^{152}Pr→^{152}Nd ($T_{1/2}$=3.8 s) [46] decays.

B. Lifetime measurement

Lifetime information was derived from $\beta\gamma$ delayed coincidences in two fast timing detectors: a 2-mm Pilot-U plastic for β rays and a cylindrical BaF_2 crystal (with a diameter of 2.5 cm and a height of 2.5 cm) for γ transitions. The ΔE β detector provided a β response almost independent of the feeding β-ray energy, while an additional γ coincidence with a Ge detector was used to select the desired decay path. Three detectors were positioned in a plane around the direct-beam collection point (parent port configuration). The BaF_2 crystal was strongly shielded from cross-scattered radiation by a combination of copper and lead absorbers. The $\beta\gamma\gamma$ coincidences were collected in cycles during deposition of the beam on the tape. After 8 s of beam collection the old source was removed and a new cycle began. Only events from the ^{152}Pr→^{152}Nd and ^{152}Pm→^{152}Sm decays were recorded as the β energy of the ^{152}Nd→^{152}Pm decay was too low to be accepted in the β gate. (The results for ^{152}Nd will

be reported in a forthcoming publication.)

Lifetimes were measured by the centroid shift technique. The mean life τ ($\tau = T_{1/2}/\ln 2$) for a level directly β fed is given by the difference between the centroid of the delayed time spectrum and the prompt centroid of the same E_γ. In the case of indirect feeding (where the level of interest is fed by a γ ray from a higher-lying level), the mean life of interest is given by the difference between the centroid shift of the spectrum gated by the deexciting γ ray and the centroid shift of the spectrum gated by the feeding γ transition.

Crucial to the centroid shift technique is the calibration of the prompt position as a function of γ-ray energy. The prompt and delayed time spectra were measured concurrently in order to maintain identical conditions in the face of small but persistent drifts of the electronics. However, as these internal prompt points were insufficient to map the prompt curve in the whole range of interest, additional information was required. It was already verified [41–43] that the shape of the prompt curve is not affected by electronic drifts although its position is shifted by a constant. The shape of the prompt curve (so-called *relative prompt* or *walk curve*) is deduced in a dedicated calibration measurement and is then shifted by a constant to overlap with prompt points internal to the decay under study. A relative prompt curve was deduced using a simple calibration procedure of Ref. [43] already applied to a number of measurements in the low-picosecond range [47, 48]. We utilized the mass separated $A = 96$ beam as the decay schemes of ^{96}Rb→^{96}Sr and ^{96}Sr→^{96}Y are simple and the lifetimes of several key levels in ^{96}Sr and ^{96}Y have been recently measured [43] with high precision.

The constant by which the relative prompt curve had to be shifted to overlap with the prompt points internal to the ^{152}Pm→^{152}Sm decay was obtained using three independent groups of data: (a) positions of Comptons from high-energy transitions (assumed to be prompt) deexciting higher-lying levels, $E_x \geq 2$ MeV, (b) positions of selected γ rays deexciting levels with known [49] lifetimes with shifts due to these lifetimes subtracted [these were levels at 366.5 keV, $T_{1/2}$=57.7(8) ps, 810.2 keV, $T_{1/2}$=7.2(6) ps, and at 963.3 keV, $T_{1/2}$=28(2) fs], and (c) full energy peaks of high-energy transitions (assumed to be prompt) deexciting the 2285.0-keV and 2042.8-keV levels. The normalization parameters were found to be consistent with each other, and thus, their averaged value was used in the further analysis.

III. RESULTS

A. Low-spin decay of ^{152}Pm →^{152}Sm

The low-lying levels in ^{152}Sm [49] have mainly been studied from the decays of ^{152}Eu [20–22, 50–52] and ^{152}Pm [53, 54]. The former decay represents a basic γ-ray energy and intensity standard, thus a number of transitions deexciting levels of spin $I \geq 2$ are known with a precision unmatched in our work. On the other hand, the low-spin decay of ^{152}Pm strongly populates levels of spins I=0 including the important 0_3^+ level at 1082.7 keV [53].

The $\gamma\gamma$ results are summarized in Table I and Fig. 2. About 15 new levels and 15 new γ transitions from the 4.1 m ^{152}Pm→^{152}Sm decay have been observed, while a number of weak transitions reported before [54] have not been confirmed. Present coincidence results allowed placing all the new and six previously unassigned γ rays into the level scheme, and also suggested new placements

TABLE I. Energies, relative intensities, and level assignments for γ rays from the β decay ^{152}Pm(4.1 min)→^{152}Sm obtained in the present study.

E_γ	I_γ (rel)	E_i (level)	E_γ	I_γ (rel)	E_i (level)
119.5(2)[a]	2.8(1)	1082.7	1086.5(4)	1.6(1)	1086.5
121.8(1)	100	121.8	1112.4(5)	0.5(1)	1234.0
209.5(6)[a]	0.13(3)	1292.5	1127.4(5)[b]	0.9(1)	2091.4
244.7(1)	6.2(3)	366.5	1253.2(6)	0.4(1)	2295.3
251.4(4)	0.9(1)	1292.5	1274.4(7)	0.3(1)	2237.2
272.5(2)[a]	2.1(1)	1082.7	1293.0(4)	1.3(1)	1292.5
329.2(3)	1.5(1)	1292.5	1317.4(5)[b]	1.3(1)	2127.7
365.9(5)[c]	0.39(4)	1658.4	1321.6(2)	6.8(4)	2284.9
443.6(3)	1.3(1)	810.1	1326.4(3)[a]	0.3(1)	2366.8
534.1(7)	0.2(1)	1768.9	1332.0(4)	0.3(1)	2295.3
563.0(2)	2.8(1)	684.8	1388.8(3)	2.5(1)	1510.6
564.1(5)	<1.0	1650.4	1403.0(6)[a]	0.5(1)	2366.8
571.9	<1.1		1408.2(5)	1.2(1)	1530.0
616.0(3)[a]	0.1(1)	2127.7	1488.1(6)[a]	0.2(1)	2172.6
642.8(3)[a]	1.0(1)	2172.6	1535.3(10)	0.2(1)	1658.4
661.7(4)	1.5(1)	2172.6	1558.5(11)	0.1(1)	1680.3
674.2(4)	2.1(1)	1040.8	1770.4(10)	0.2(1)	1768.9
688.3(4)	3.7(2)	810.1	1822.1(6)	0.6(1)	1944.1
695.9(3)	16.6(8)	1658.4	1843.2(10)	0.1(1)	1965.0
727.1(7)[a]	0.2(1)	2237.2	1873.1(10)	0.1(1)	2239.7
735.1(3)	3.3(2)	1776.1	1921.6(10)	0.1(1)	2043.0
810.2(3)	1.6(1)	810.1	1970.8(9)	0.3(1)	2091.4
812.9(3)	3.0(2)	1776.1	2007.0(5)[a]	1.1(1)	2127.7
841.4(2)[d]	25.8(13)	963.3	2045.2(6)	0.8(1)	2167.0
847.5(5)[a]	0.4(1)	1658.4	2053.9(10)[a]	0.2(1)	2175.7
861.7(8)[a]	0.1(1)	1944.1	2079.3(4)	2.9(2)	2201.2
867.2(5)	0.4(1)	1234.0	2114.2(8)[a]	0.2(1)	2237.2
870.2(4)	0.7(1)	1680.3	2118.0(3)	1.3(1)	2239.7
903.3(5)	0.7(1)	1944.1	2165.6(10)	0.2(1)	2287.4
919.0(2)	5.3(3)	1040.8	2175.0(8)	0.4(1)	2295.3
926.0(3)	3.1(2)	1292.5	2187.0(6)	0.5(1)	2308.9
929.1(4)	1.3(1)	1892.4	2224.8(5)[b]	2.3(1)	2224.8
958.2(4)	0.3(1)	1768.9	2239.7(8)	0.4(1)	2239.7
960.9(2)	23.4(12)	1082.7	2255.0(15)[a]	0.1(1)	2376.8
963.3(2)	22.7(11)	963.3	2309.1(9)	0.4(1)	2308.9
981.0(3)	1.4(1)	1944.1	2387.9(10)	0.4(1)	2509.7
995.7(5)	0.6(1)	1680.3	2566.0(10)[b]	0.4(1)	2687.8
1050.0(4)[b]	1.0(1)	2091.4	2803.7(10)[b]	0.5(1)	2925.5
1079.5(3)	3.7(2)	2043.0			

[a] Gamma transition not earlier reported from this decay.
[b] Gamma transition not earlier placed in the level scheme.
[c] Tentative assignment to ^{152}Sm.
[d] The absolute intensity of this γ ray was measured by Daniels and Hoffmann [55] to be 3.2(3)% per decay.

for some of the transitions seen before.

The γ-ray energies and intensities, listed in Table I, were deduced from both the γ singles and the $\gamma\gamma$ results. The small intensity contributions to some of the γ transitions common to the decays of the 7.52 and 13.8 min isomers of ^{152}Pm [49] were calculated and subtracted from the measured intensities. Our transition energies agree very well with those of Ref. [53] and the precise energies compiled in Ref. [49]. However, there are strong (and presently unexplained) systematical differences between energies presented here and those of Ref. [54] for $E_\gamma \geq 1.8$ MeV.

The revised I_β and $\log ft$ values are shown in Fig. 2. The β intensities were normalized by using the value of I_γ=3.2% per decay of ^{152}Pm for the 841.4-keV γ transition [55], leading to a 17% β feeding of the 2_1^+ level. Relatively weak $E0$ intensities were not included in the calculation of the β intensities.

The important new features of the revised level scheme are the 119.5-, 209.5-, and 847.5-keV lines deexciting the 1082.7-, 1292.5-, and 1658.4-keV states, respectively. Moreover, the 272.5-keV transition from the 0_3^+ level has not been previously observed from the ^{152}Pm decay. The 1650.6-keV level seems to be weakly populated as evinced by the 564.1-keV transition observed in the $\gamma\gamma$ coincidences. However, the 415.5-keV transition is not seen in this work, while the 1528.0-keV transition, earlier reported to deexcite the 1650.6-keV level, seems to have a $T_{1/2}(\beta^-) \approx 4$ s, and may thus belong to the decay of ^{152}Pr.

TABLE II. Level lifetimes in ^{152}Sm deduced in the present study.

Level (keV)	$T_{1/2}$ (ps)
1040.8	<16
1082.7	15(6)
1292.5	<16
1658.4	8(5)
1776.1	<15

The new lifetime results, which are listed in Table II, represent averages over a few independent results obtained by selecting, for example, different transitions deexciting the same level. In particular, the lifetimes of

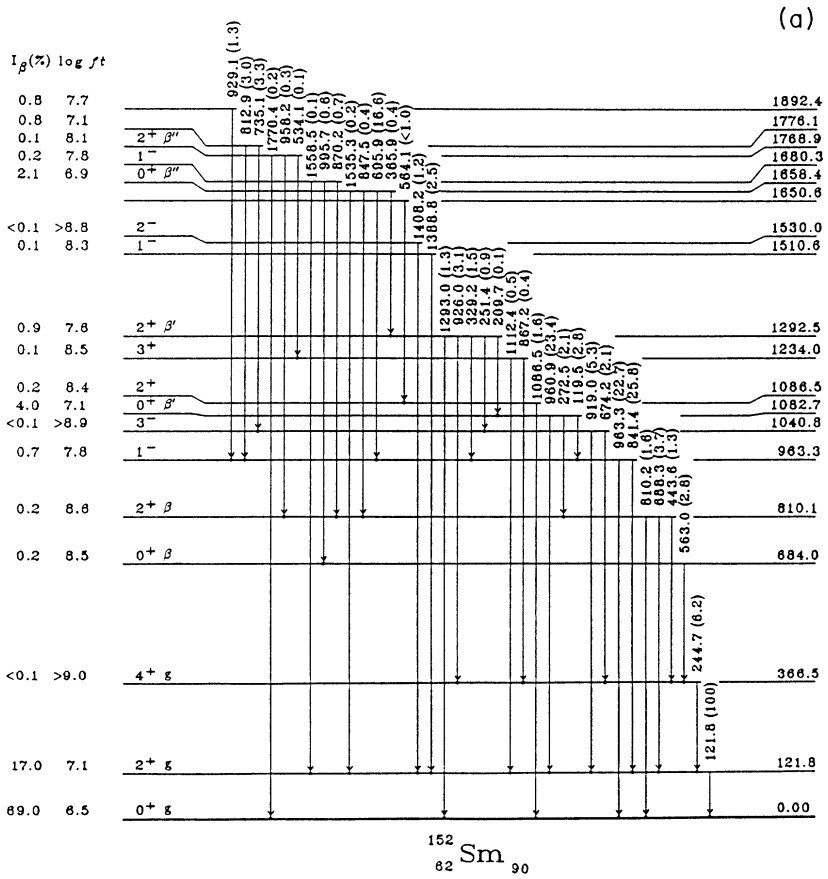

FIG. 2. Level scheme for the low-spin decay of ^{152}Pm→^{152}Sm (a) low-energy part, and (b) higher energies. Spin assignments are from Ref. [49]. Labels g, β, γ, β', and β'' mark members of various bands discussed in the text. The figure is not drawn to scale.

the 1082.7- and 1658.4-keV levels were averaged over five independent results.

B. β' band in ^{152}Sm

The transition rates deduced for the 0_3^+ band (labeled β') are presented in column 2 of Table III. The absolute rates for the $0^+_{\beta'}$ level at 1082.7 keV are obtained from the level lifetime and the γ intensities measured in this work, while those for the $2^+_{\beta'}$ level at 1292.5 keV are calculated from the branching ratios of Ref. [49] by adjusting the $\rho^2(E0;\ 2^+_{\beta'} \rightarrow 2^+_{\beta})$ rate to equal that of the $0^+_{\beta'} \rightarrow 0^+_{\beta}$ transition. This assumption, generally valid in deformed nuclei [1], needs to be approximately valid here as the statistical uncertainty of this normalization is $\sim 50\%$.

Nevertheless, to check this assumption we have used the simplest rotational model in the adiabatic approximation [1] to predict the absolute transition rates for the $2^+_{\beta'}$ state based on the transitions rates from the $0^+_{\beta'}$ bandhead:

$$B(E1; K=0, I_i \rightarrow K=0, I_f) = < I_i 010 \mid I_f 0 >^2 \mid M_{if}^{E1} \mid^2,$$

$$B(E2; K=0, I_i \rightarrow K=0, I_f) = < I_i 020 \mid I_f 0 >^2 \mid M_{if}^{E2} \mid^2 .$$

In these formulas I_i, I_f, and M_{if} represent the spins of the initial and final levels and the matrix element between the bands, respectively. Out of eight model predictions for the $2^+_{\beta'}$ level (column 3 of Table III) six are rather reasonable (within a factor of 2) giving support to the aforementioned assumption of equal $E0$ strengths.

Transition rates for the low-lying bands in ^{152}Sm have been calculated by Kumar [3] with the pairing-plus-quadrupole model. These microscopic PPQ calculations provide a test of the shape-coexistence hypothesis for ^{152}Sm as the shape coexistence is not presupposed but could come out naturally from the calculations. It was already shown [3] that various calculated results including the $B(E2)$ and $\rho^2(E0)$ rates compare well with the experimental values for the lower-lying g.s., β, and γ bands. However, the results for the "mixed" 0_3^+ band (not experimentally tested so far) represent the most controversial outcome of the Kumar calculations.

The experimental and calculated results for the 0_3^+ band are listed in columns 2 and 4 of Table III, respec-

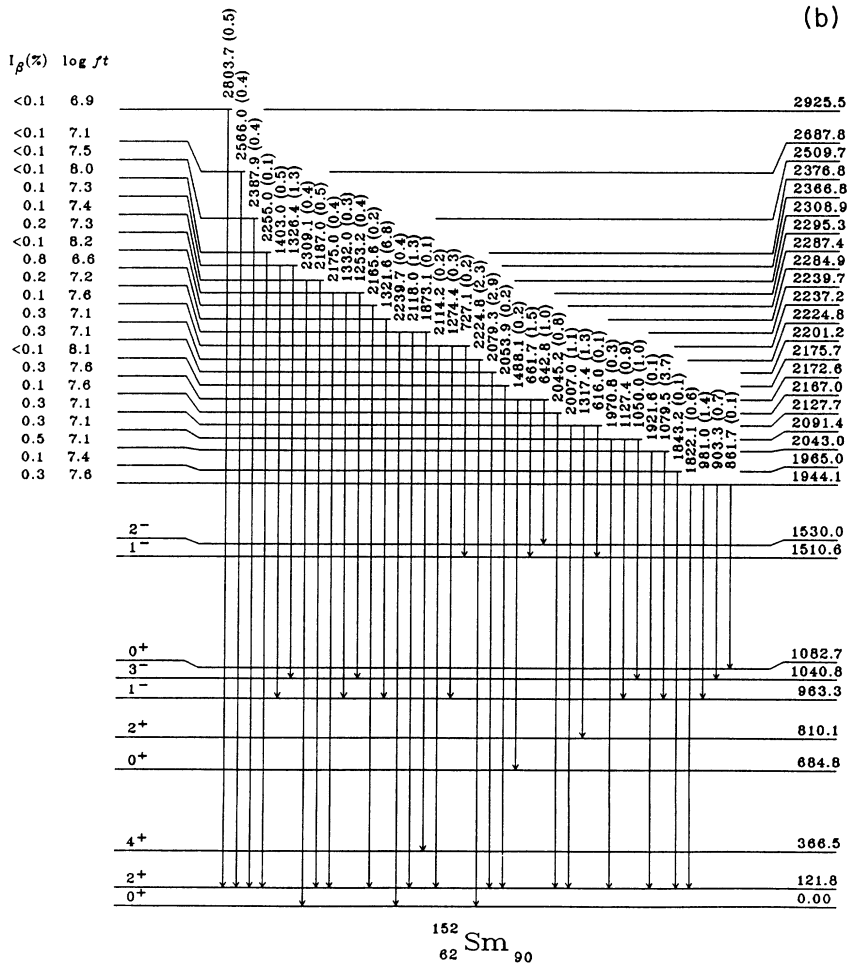

FIG. 2. (*Continued*).

tively. There is good agreement in all but one case: the $\rho^2(E0; 0^+_{\beta\prime} \rightarrow 0^+_{\beta})$ rate is overestimated by a factor of 10. The experimental data support the calculations, which do not yield for this nucleus (long interpreted [14, 16–19] as a classical case of shape coexistence) a potential energy surface with two minima (one deformed and one spherical) or an excited 0^+_3 state with much smaller $\beta_{\rm rms}$ than the g.s. In fact, the $\beta_{\rm rms}$ calculated for the *mixed* 0^+_3 band is almost the same as that for the deformed g.s. band. Thus, if the model of Kumar is to be believed, there is no shape coexistence in ^{152}Sm, and by logical conclusion, in the transitional Sm nuclei. A note of caution: the excitation energies for the 0^+, 2^+, and 4^+ levels of the *mixed* 0^+_3 band are calculated [3] as 1473, 1839, and 2210 keV — above the measured energies of 1083, 1293, and (1613) keV, respectively. Furthermore, although the model worked remarkably well in various regions, it predicted [3, 7] poorly the $B(E2)$ branching ratios for the low-lying bands in ^{150}Sm. However (see Sec. IV D), the absolute $B(E2)$ rates in the original [3] and in the revised [6, 7] calculations seem to be quite reasonable.

So far, transition rates for the β' band in ^{152}Sm have not been calculated with the shape-coexistence model. The 0^+_3 bands in heavy Sm and Gd are considered outside the model space for the IBA calculations [58], but these bands (labeled *intruder*) can be treated using the mixing (shape-coexistence) IBA model [12] where two standard IBA configurations, one explicitly less deformed than the other, are allowed to interact and mix. Unlike the microscopic PPQ model, which demonstrates its predictive power, the shape-coexistence phenomenological models have parameters which are not determined microscopically, but are generally deduced *post factum* by adjusting them to the known data.

The PPQ calculations indicate that the $E0$ and $E2$ transition rates in ^{152}Sm can be explained without involving shape coexistence. These surprising results would fall in line with those of Fahlander *et al.* [26] provided that the low-lying bands in Sm, including the 0^+_3 band, evolve from the quadrupole phonon multiplets in a shape independent way. Indeed, such an evolution appears to be observed in the systematics of heavy Sm and Gd discussed in Sec. IV. In this picture the 0^+ and 2^+ states of the 0^+_3 band evolve from the 0^+ $N = 3$ and 2^+ $N = 4$ vibrational states. However, one could also ask whether there are any other 0^+ bands in ^{152}Sm that would fit within the same framework of interpretation?

TABLE III. Experimental and theoretical $B(E2)$, $B(E1)$, and $\rho^2(E0)$ rates for transitions deexciting the β' and the β'' bands in ^{152}Sm.

$I_i \rightarrow I_f$	Experimental[a]	RM[b]	PPQ[c]
	$B(E2)$ (W.u.)		
$0_{\beta'} \rightarrow 2_g$	0.8(3)	(0.8)	3.0
$2_{\beta'} \rightarrow 0_g$	0.21(11)	0.16	0.7
$2_{\beta'} \rightarrow 2_g$	0.11(6)	0.22	0.07
$2_{\beta'} \rightarrow 4_g$	2.7(14)	0.40	1.5
$0_{\beta'} \rightarrow 2_\beta$	40(16)	(40)	82
$2_{\beta'} \rightarrow 0_\beta$	$\leq$0.5	8.0	0.34
$2_{\beta'} \rightarrow 2_\beta$	9(5)	11	8.4
$2_{\beta'} \rightarrow 4_\beta$	40(21)	20	34
$2_{\beta'} \rightarrow 0_{\beta'}$	184(100)	78[d]	96
$0_{\beta''} \rightarrow 2_g$	0.0021(15)		
$0_{\beta''} \rightarrow 2_\beta$	0.08(5)		
$0_{\beta''} \rightarrow 2_\gamma$	<1.4		
$0_{\beta''} \rightarrow 2_{\beta'}$	5^{+7}_{-2}		
	$10^3\rho^2(E0)$[e]		
$0_\beta \rightarrow 0_g$	83(9)		133
$0_{\beta'} \rightarrow 0_g$	1.2(8)		1.4
$0_{\beta'} \rightarrow 0_\beta$	21(9)		195
$2_{\beta'} \rightarrow 2_\beta$	(21)		153
	$B(E1)$ (10^4 W.u.)		
$0_{\beta'} \rightarrow 1^-_1$	9(3)	(9)	
$2_{\beta'} \rightarrow 1^-_1$	5(2)	4	
$2_{\beta'} \rightarrow 3^-_1$	6(3)	5	
$0_{\beta''} \rightarrow 1^-_1$	0.9(5)		

[a] Transition rates from the $2_{\beta'}$ state are normalized in a model dependent way, see text. The total uncertainty includes 50% uncertainty due to normalization.

[b] Simplest rotational model, see text.

[c] Pairing-plus-quadrupole model, Ref. [3].

[d] Deduced from $E_\gamma = E_{2+} - E_{0+}$=210 keV and the best global fit of Ref. [56].

[e] $\rho^2(E0)$ deduced using the electronic factors Ω from Ref. [57].

C. Higher-lying 0^+ bands in ^{152}Sm

Transition rates deduced for the 0^+_4 state at 1658.4-keV (labeled β'') are presented in column 2 of Table III. One observes strongly retarded $B(E2)$ rates to the 2^+_g and 2^+_β states and rather low $B(E2)$ and $B(E1)$ rates to the 2^+_γ and 1^-_1 state, respectively. Based on a weak 365.9-keV γ ray (tentatively assigned to this decay) we deduce the $B(E2; 0^+_{\beta\prime\prime} \rightarrow 2^+_{\beta\prime})$ rate of 5^{+7}_{-2} W.u. which implies that the strongest link exists between the β'' and the β' bands. It seems that the 1658.4-keV level is neither the two-phonon β bandhead nor the 0^+ state evolving from the N=4 quadrupole phonon multiplet. The latter state would be characterized by very slow $B(E2)$ rates to the 2^+_γ and 2^+_g levels and a fast one ($\Delta N = 1$) to the 2^+_β state. Based on the limited experimental data, the observed $B(E2)$ pattern appears to be consistent with interpretation of the 0^+_4 state as the 0^+ state of the $N = 5$ multiplet. A 2^+ level at 1768.9 keV could be the 2^+ member of the 0^+_4 band. The energy difference, E_{2+} –

E_{0+}, of 110 keV is reasonably close to the value of ~123 keV for the g.s. and β bands.

Out of five known 0^+ states (all below 1.8 MeV) only the 0^+ state at 1736(5) keV [59] has not been observed in the β^- decay of Pm. Three states, 0_1^+, 0_3^+ and 0_4^+, are preferentially β fed with logft values of 6.5–7.1, while two states, 0_2^+ and 0_5^+, are populated very weakly or not at all. The logft to the 0_2^+ state is as high as 8.5, and even higher if allowing for unobserved γ transitions, and the β feeding to the 0_5^+ state seems to be equally hindered.

This high selectivity of the β^- decay is matched by the selectivity of the (p,t) [and perhaps also of the (t,p)] reactions. The 0^+ states strongly populated in the β^- decay are barely populated in the (p,t) reaction [15, 16, 18, 19, 59] and vice versa. Besides the g.s., the (p,t) reaction strongly populates the 0_2^+ state while the population of the 0_5^+ level is rather modest [59]. On the other hand, the (t,p) reaction [14] populates the 0_3^+ state with an exceptional strength. Unfortunately, the population of the higher-lying 0^+ states is not presently known.

To summarize this section, a strong similarity is manifested in the population pattern for the 0_2^+ (β) and 0_5^+ states, and independently for the 0_3^+ (β') and 0_4^+ states. These two complementary patterns appear to emphasize strong differences in the intrinsic structures of the 0_2^+ and 0_3^+ states. With the data at hand, it would be too speculative to interpret the 0_5^+ and 0_4^+ states as evolving from the 0^+ vibrational states with $N = 4$ and $N = 5$, respectively. We also note, that the strong population of the 2284.9-keV state in the β^- decay (logft=6.6) and its decay pattern make this state a J^π=0^+ candidate.

IV. BAND SYSTEMATICS FOR HEAVY SM AND GD ISOTOPES

A. Classification of levels

We now examine the energy and transition rate systematics of the 0^+ bands in the heavy Sm and Gd nuclei against the schematic (shape coexistence and correspondence) interpretations. We have chosen the population in the (p,t) and (t,p) reactions to provide a consistent and independent classification of the excited 0^+ states. A sequence of states strongly populated in the (p,t) reaction and weakly in the (t,p) transfer is labeled β (as levels of this sequence were recognized in Sm [3] and other nuclei [60] as the β bandheads). An alternative sequence with the opposite features is labeled β'. Figure 3(a) shows the excitation energies of the β and β' states, demonstrating a strong similarity between Sm and Gd isotones — a feature that is explored further in this section. Our labeling, which is based on the intrinsic level properties, differs from that of Sakai [32] who marked as β and β' consecutively the first and the second excited 0^+ bands. Yet, for the heavy Sm and Gd nuclei these labeling schemes are identical except for $N = 94$, where our β' band is positioned below the β band (see Fig. 3). This interchange of the 0^+ bands in ^{158}Gd has been noted [60, 62] before.

The 0^+ sequences defined above overlap with the β and β' bands of the correspondence interpretation (see Fig. 1) provided (which is critical here) that the "shape-coexisting" β' bands can be treated as part of these dynamically evolving phonon multiplets. In general, the level systematics show smooth changes with the possible exception of the "intruder" states. However, the excitation energies for the β' sequence [see Fig. 3(a)] remain almost constant unaffected by the discontinuities at $N = 88/90$, while the excitation energy for the β sequence changes widely. This reaffirms that the β and β' sequences have different intrinsic structures as already seen from the (p,t) and (t,p) reactions and in the β^- decay discussed above.

In the shape-coexistence interpretation [12, 14, 16–19] two intrinsically different configurations (spherical and deformed) coexist in a nucleus. The *spherical* sequence includes the g.s. bands for $N \leq 88$ and the β' (0_3^+) bands for $N \geq 90$, while the *deformed* sequence includes the β' (0_3^+) band for $N = 88$ and the g.s. bands for $N \geq 90$. (The β' levels, which at $N = 88$ and 90 have been interpreted [14–18] as shape-coexisting levels, were assumed to retain this role at $N = 92$–94.) The resultant systematics [Fig. 3(b)] shows a sharp level crossing at $N = 88/90$.

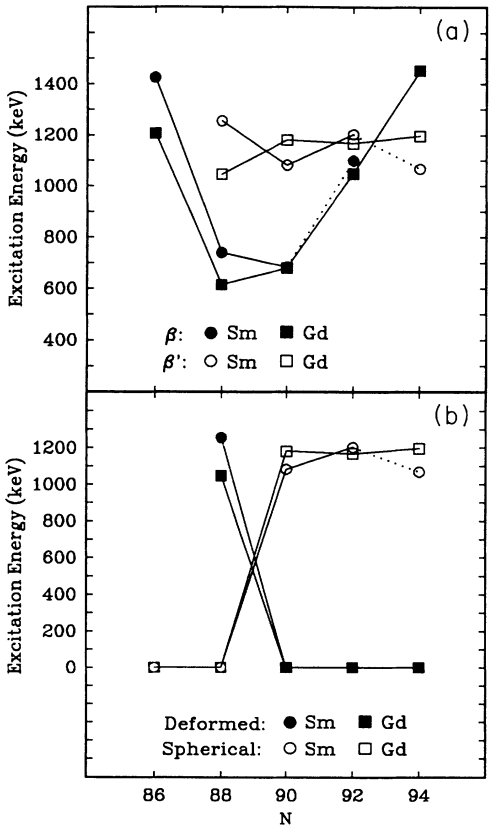

FIG. 3. (a) Excitation energies of the β (solid markers) and β' (open markers) sequences of 0^+ states in heavy Sm (circles) and Gd (squares). In cases where no (p,t) data exist, levels are connected by dotted lines based on the pattern of systematics. Data are from Refs. [32, 61]; see the text for ^{154}Gd. (b) Same as (a) but for the *deformed* (solid markers) and *spherical* (open markers) sequences of 0^+ states.

B. Energy systematics within 0^+ bands

We now examine the relative level energies within the band sequences. In the correspondence interpretation (Fig. 4) all three 0^+ bands evolve towards rotational patterns characteristic of a deformed structure. The fact that the (intruder) β' and the other two bands show similar behavior strongly supports the correspondence interpretation. On the other hand, discontinuities observed at $N = 88$ and 90 provide an argument for the alternative interpretation as no such discontinuities can be seen in the *spherical* and *deformed* band systematics illustrated in Figure 5.

The *deformed* sequence in Sm has been previously considered by Debenham and Hintz [19]. They found the ratio R of the relative 4^+ and 2^+ energies to be consistently ~3.3 and concluded that each band in this sequence is well deformed. Our much updated systematics [Fig. 5(b)] differs with that of Ref. [19] at two points: it excludes the 0_2^+ band in ^{148}Sm which we classify as β, while for ^{150}Sm it includes two 4^+ levels (at 1642.6 and 1819.5 keV) which seem to share the population and decay properties of the *deformed* 4^+ state. (These levels

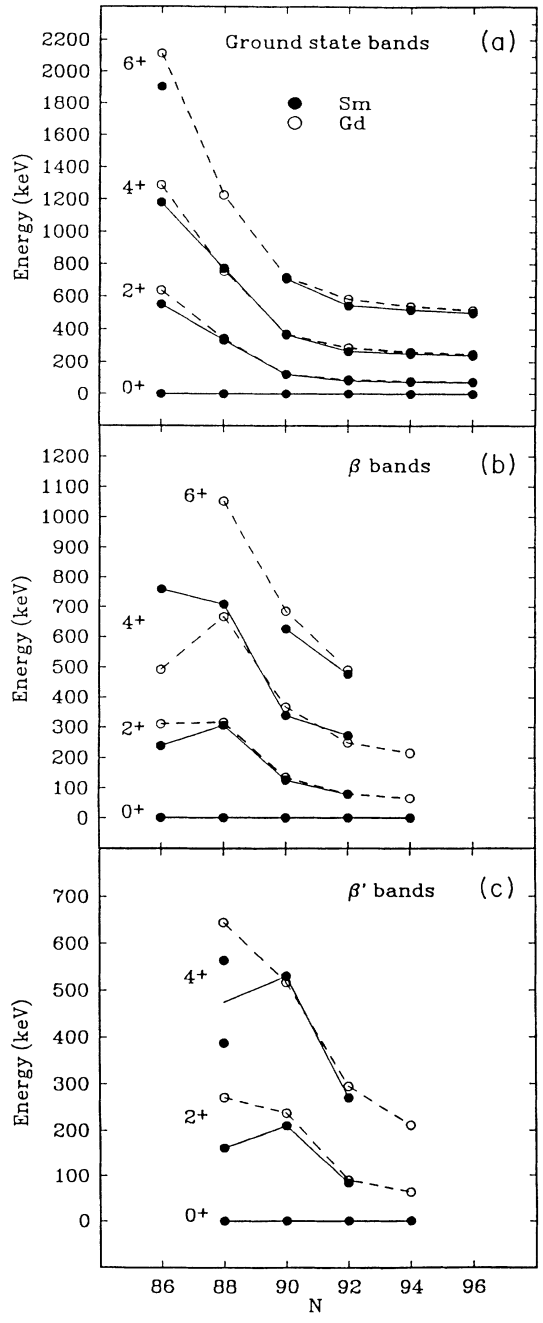

FIG. 4. Relative excitation energies within the ground state, β, and β' sequences of bands in heavy Sm (solid circles connected by solid lines) and Gd (open circles connected by broken lines). Note discontinuities at $N = 88/90$ for the β and β' bands. Data are from Refs. [32, 61]; see the text for ^{154}Gd.

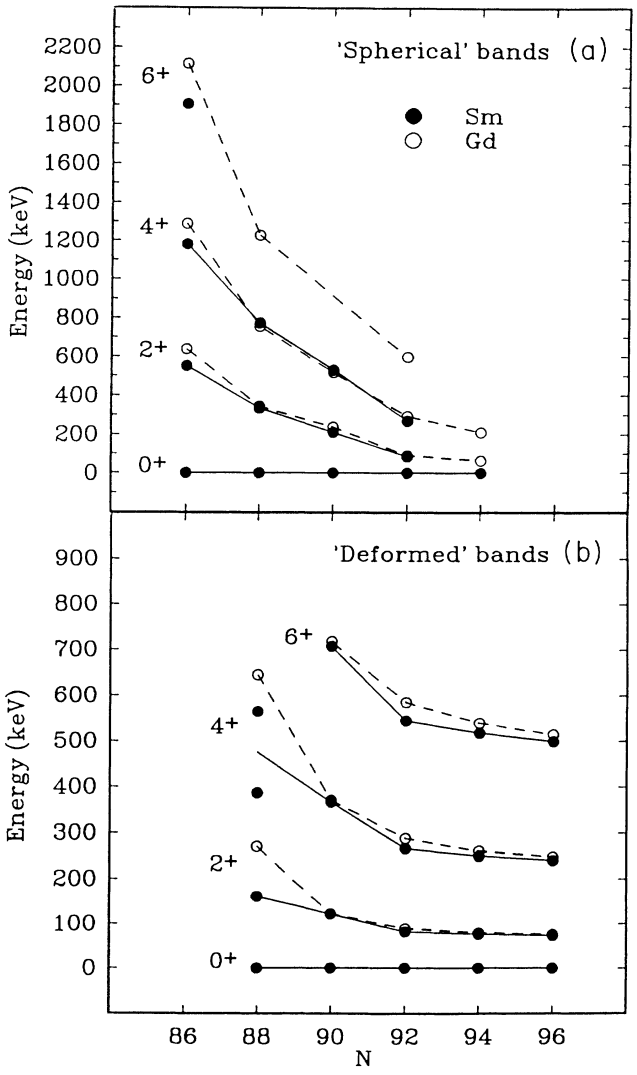

FIG. 5. Relative excitation energies within the *deformed* and *spherical* sequences of bands in heavy Sm (solid circles connected by solid lines) and Gd (open circles connected by broken lines). Data are from Refs. [32, 61]; see the text for ^{154}Gd.

are placed at the relative energies $E_{2+} - E_{0+} = 387.1$ and 564.0 keV.) As a consequence of the smooth decrease of the relative 2^+, 4^+, and 6^+ energies and the increase of the energy ratios R ($R \simeq 2.8$, 3.01, 3.25, 3.29 for $^{150-156}$Sm and 2.39, 3.01, 3.24, 3.29 for $^{152-158}$Gd), we conclude that the deformation of these bands changes smoothly from moderately deformed at $N = 88$ to fully deformed at $N = 96$.

The *spherical* systematics [Fig. 5(a)], which have not been considered before, also show smooth and rapid evolution towards deformation. Bands from this sequence become deformed already at $N = 92$ ($R \sim 3.3$), barely two neutrons away from $N = 90$ where they were considered spherical ($R \sim 2.2$–2.5). This trend is evident from both the 2^+ energies ($E_{2+} - E_{0+}$) and the R ratios of 2.15, 2.31, 2.52, and 3.23 for $^{148-154}$Sm, and 2.02, 2.19, 2.19, 3.27, and 3.30 for $^{150-158}$Gd.

These unexpected features clearly disagree with the shape-coexistence interpretation which presupposes either stable spherical and deformed shapes, or at least clearly defined shape differences. As the *spherical* and the *deformed* sequences evolve towards fully rotational patterns, at the point of shape transition, $N = 88/90$, both sequences are themselves in a transitional stage. Only at $N = 84$–90 does the *spherical* band sequence appear to be significantly less deformed than the *deformed* one. Consequently, the usefulness of the shape-coexistence concept seems limited. To conclude, the correspondence interpretation is the only one consistent with the data of Figs. 4 and 5.

Before we extend the discussion to the absolute transition rates we want to clarify one of the contended level assignments. Three different 0^+ levels, at 1182, 1293.1, and 1295.8 keV were assigned by different authors [63–66] as the (*spherical*) $0^+_{\beta'}$ state in ^{154}Gd. Only the 1182-keV level follows [63, 67, 68] the expected β' pattern [strongly populated in the (t,p) and weak in the (p,t) reactions] which gives direct evidence for its existence and nature. However, as the 1182-keV level was not reported in the γ spectroscopy studies [66, 69, 70], we tentatively identify the previously unassigned 1058.1(6)-keV transition (from the $J = 0$ decay of ^{154}Tb [66]) as the $0_3^+ \rightarrow 2_1^+$ ($0^+_{\beta'} \rightarrow 2^+_g$) transition and the weak 237.0-keV line [64, 70] as the $2^+_{\beta'} \rightarrow 0^+_{\beta'}$ transition. On the other hand, there is no clear evidence for any of the 1294-keV levels. A new study of the ^{154}Tb decay could clarify this issue.

C. Correspondence interpretation of the $B(E2)$ Rates

In a recent study [26] of ^{114}Cd, the $B(E2)$ rates from the rotational intruder band were found to be part of the decay pattern of a vibrational-like structure involving levels up to the 4-quadrupole phonon multiplet. This surprising result could be even more pronounced in a sequence of transitional Sm and Gd nuclei, where the $B(E2)$ rates, including those from the "shape-coexisting" β' band, should change smoothly from those of a vibrator to those of a rotor following schematic correspondence patterns. Three distinctive $B(E2)$ patterns are expected: *fast* (consistently high rates at ~50–100 W.u.), *slow* (consistently low rates at ≥ 1 W.u.), and *transitional* — a smooth decrease of transition rates by ~2 orders of magnitude from ~ 100 to ~1 W.u. The *fast* patterns involve $\Delta N = 1$ transitions in the vibrational limit (see Fig. 1) which evolve towards fast intraband transitions in the rotational limit. The *slow* patterns involve transitions forbidden in the vibrational limit (e.g., ΔN=2 transitions) which evolve towards slow interband transitions. Finally, the *transitional* patterns involve fast ΔN=1 transitions which evolve towards the slow interband transitions in the deformed region. Level mixing may alter these patterns.

The important aspect of the correspondence interpretation of the transitional (Sm and Gd) nuclei is that no distinction is made for the intruder states. Moreover, each $B(E2)$ rate should follow one of the three patterns mentioned above that is predetermined by the position of the transition in the scheme of Fig. 1. As for the shape-coexistence interpretation, no schematic pattern of $B(E2)$ rates can be provided as the implied strong mixing of the normal and intruder states complicates the simple unmixed patterns.

On the experimental side, a relatively complete set of the $B(E2)$ rates has been measured [49, 70–76] for the g.s., β, and γ bands. The results for the β' bands are scarce [75, 76], and consequently some of the absolute rates have been approximately deduced from the relative rates. As long as the approximated results fall within a factor of 2–3 of the true values, this is sufficient to identify those transitions which rates stay constant and those which rates change as a result of the shape transition. Moreover, transitions are taken to be pure $E2$ in cases when the $M1/E2$ mixing is experimentally unknown. For slow $B(E2)$ transitions, like $2^+_{\beta'} \rightarrow 2^+_g$, the $M1$ component could be dominant [77] and the true $B(E2)$ rate be lower than the rate adopted here. Such differences would not, however, alter our conclusions.

The $B(E2)$ rates for the β band (Fig. 6) feature the expected *transitional* ($0^+_\beta \rightarrow 2^+_g$ and $2^+_\beta \rightarrow 4^+_g$), *fast* ($2^+_\beta \rightarrow 0^+_\beta$), and *slow* ($\Delta N$=2, $2^+_\beta \rightarrow 0^+_g$) patterns. The exception is the (ΔN=2) $2^+_\beta \rightarrow 2^+_g$ pattern predicted to be *slow*, but where the $B(E2)$ rates vary from low values (~1 W.u.) in both limits to rather high values (~17–68 W.u.) in the transitional region in between.

The rate systematics for the γ band (Fig. 7) shows the expected *fast* and *transitional* patterns for the $4^+_\gamma \rightarrow 2^+_\gamma$ and the $2^+_\gamma \rightarrow 2^+_\beta$ transitions, respectively. On the other hand, the overall pattern for the $2^+_\gamma \rightarrow 0^+_g$ transition is *slow*, as expected, but at somewhat higher $B(E2)$ rates of ~3 W.u. A more serious discrepancy is observed for the $2^+_\gamma \rightarrow 2^+_g$ pattern expected to be *transitional*. The *transitional* pattern is approximately followed in Gd, while in Sm the pattern is rather flat with $B(E2)$ rates of ~8 W.u. (at N=86–88), which is lower than the expected rates of ~40–100 W.u. The lower rates in this case seem to be correlated and somewhat complementary to the higher rates observed for the 2^+_β state in Fig. 6(d).

Figure 7 includes three approximated results obtained by assuming constant rates for the *slow* transitions. In

^{150}Gd the $B(E2;\ 2^+_\gamma \rightarrow 2^+_g)$ rate of ~78 W.u. was obtained by fixing the $B(E2;\ 2^+_\gamma \rightarrow 0^+_g)$ rate to ~2 W.u. The latter value was selected from seven $B(E2;\ 2^+_\gamma \rightarrow 0^+_g)$ rates measured for $^{148-154}$Sm and $^{154-158}$Gd that range from 1.7 to 6.0 W.u. In ^{154,158}Gd the $B(E2;\ 4^+_\gamma \rightarrow 2^+_\gamma)$ rates of ~86 and ~100 W.u., respectively, were obtained by setting the $B(E2;\ 4^+_\gamma \rightarrow 2^+_g)$ rates to 1 W.u. The latter value represents an average of the $B(E2;\ 4^+_\gamma \rightarrow 2^+_g)$ rates of 0.7(3) W.u. for ^{152}Sm and 1.3(2) W.u. for ^{156}Gd.

In the case of the β' systematics the absolute transition rates have been measured for the $0^+_{\beta'}$ state in ^{152}Sm (this work), for the $0^+_{\beta'}$ and $2^+_{\beta'}$ states in ^{156}Gd [75], and for the $2^+_{\beta'}$ state in ^{158}Gd [76]. For ^{150}Sm and ^{152,154}Gd the absolute rates were approximated: first for the $2^+_{\beta'}$ state by setting the fast intraband $B(E2;\ 2^+_{\beta'} \rightarrow 0^+_{\beta'})$ rate equal to 110, 100, and 200 W.u., respectively, and then for the $0^+_{\beta'}$ state by setting the $\rho^2(E0;\ 0^+_{\beta'} \rightarrow 0^+_\beta)$ and $\rho^2(E0;\ 2^+_{\beta'} \rightarrow 2^+_\beta)$ rates equal.

The resultant systematics are shown in Table IV. Uncertainties (expected to be large) are not provided for the approximated results. Rather steady rates are observed in most cases, which provides support to the approximations used. Large fluctuations are observed for the very retarded $B(E2;\ 2_{\beta'} \rightarrow 0_g)$ and $B(E2;\ 2_{\beta'} \rightarrow 2_g)$ transitions with no effect on the final conclusions. There are six $B(E2)$ patterns that follow the expectations: one *fast* for the $2^+_{\beta'} \rightarrow 0^+_{\beta'}$ transition and five *slow* for the $0^+_{\beta'} \rightarrow 2^+_g$, $2^+_{\beta'} \rightarrow 0^+_g$, $2^+_{\beta'} \rightarrow 2^+_g$, $2^+_{\beta'} \rightarrow 4^+_g$, and $2^+_{\beta'} \rightarrow 0^+_\beta$ transitions, while two sequences involving (again) the 2^+_β and 2^+_γ states somewhat deviate from the expected patterns. By now this deviation is fully expected, and, in

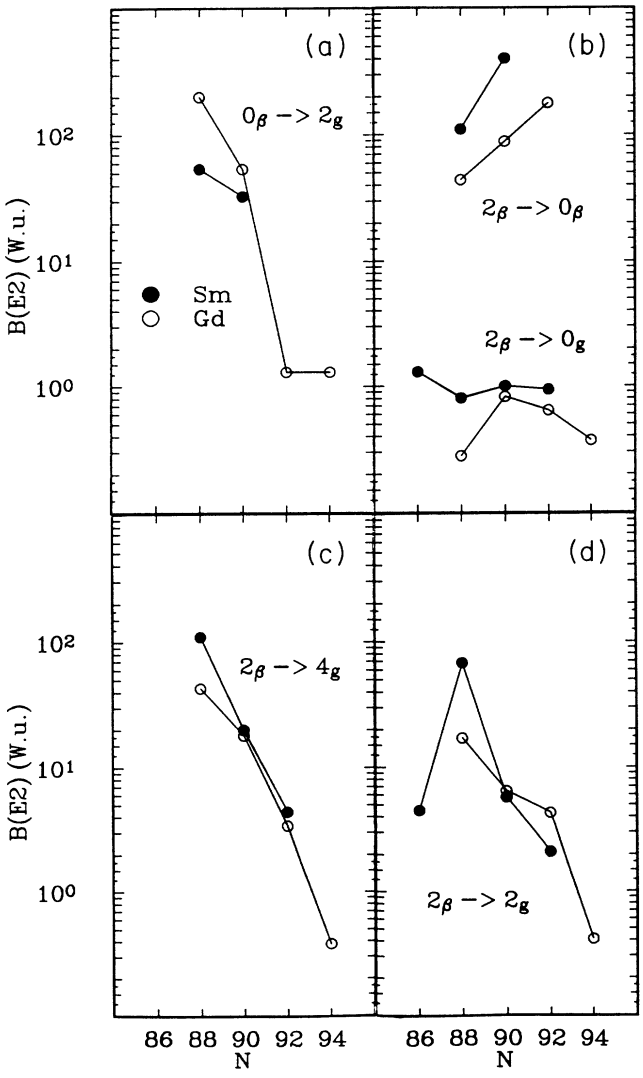

FIG. 6. $B(E2)$ systematics for the intraband $\beta \rightarrow \beta$ and interband $\beta \rightarrow$ ground-state transitions in the heavy Sm (filled circle) and Gd (open circle) nuclei. Data are from Refs. [49, 70–76].

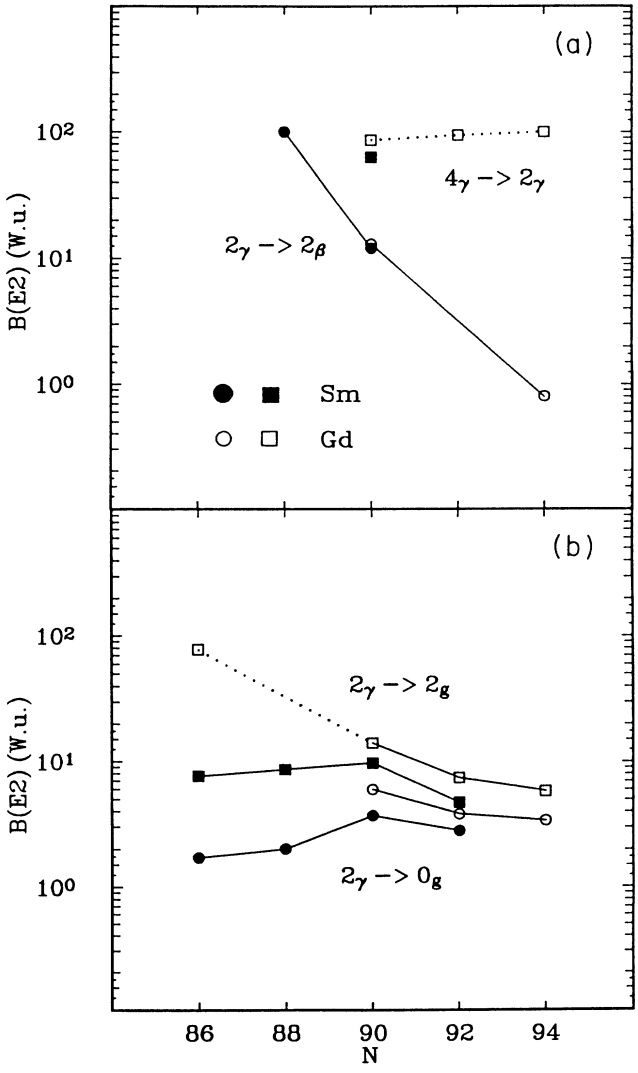

FIG. 7. (a) $B(E2)$ systematics for the intraband $4_\gamma \rightarrow 2_\gamma$ (squares) and interband $2_\gamma \rightarrow 2_\beta$ (circles) transitions in heavy Sm (filled markers) and Gd (open markers) nuclei. (b) Same as (a) but for the $2_\gamma \rightarrow 0_g$ (circles) and $2_\gamma \rightarrow 2_g$ (squares) transitions. Data are from Refs. [49, 70–76].

fact, necessary if the data are to be self-consistent. The apparent "mixing effect" of the 2_γ^+ and 2_β^+ states is to lower the fast *transitional* and *fast* rates and to raise the *slow* rates. Indeed, this effect is seen for the $2_{\beta'}^+ \rightarrow 2_\beta^+$ transition. Our data for N=88 and 90 show $B(E2)$ rates at 9–16 W.u., lower than the expected *transitional* rate of 40–100 W.u. Similarly, significantly higher values of 13–21 W.u. are observed for the $2_{\beta'}^+ \rightarrow 2_\gamma^+$ transition predicted to be *slow* at ~1 W.u.

To summarize, the $B(E2)$ rates observed for the β, γ, and β' bands generally follow the correspondence interpretation. Almost all of the discrepancies can be traced to the "mixing effect" of the 2_β^+ and 2_γ^+ states in the transitional region. The explanation of these discrepancies, of the pattern of E0 rates, and of the relatively high $B(E2)$ rates of ~40 W.u. observed for the (ΔN=0) $0_{\beta'}^+ \rightarrow 2_\beta^+$ and $2_{\beta'}^+ \rightarrow 4_\beta^+$ transitions, requires a detailed model analysis which is beyond the scope of this work. At least for ^{152}Sm, the $B(E2)$ and $E0$ rates are well reproduced by the PPQ model [3].

D. Mixing effect in ^{150}Sm

The "mixing effect" is also critical to the PPQ model which failed [3] to account for the $E2$ branching ratios in ^{150}Sm [3, 6, 7]. The problem was traced [6, 7] to the delicate balance between pairing and quadrupole forces in a softly deformed ^{150}Sm and was corrected in the dynamic PPQ (DPPQ) calculations [6, 7] (see Table V).

TABLE IV. Systematics of the experimental $B(E2)$, $B(E1)$, and $\rho^2(E0)$ rates from the β' band in the heavy Sm and Gd nuclei. Data from Refs. [49, 62, 70, 64, 71–76, 78, 79] and Table III. Some values depend on the normalization procedure, see text.

$I_i \rightarrow I_f$	^{150}Sm$_{88}$	^{152}Sm$_{90}$	^{152}Gd$_{88}$	^{154}Gd$_{90}$	^{156}Gd$_{92}$	^{158}Gd$_{94}$
			$B(E2)$ (W.u.)			
$0_{\beta'} \rightarrow 2_g$	0.17	0.8(3)	1.4		3.4(10)	
$2_{\beta'} \rightarrow 0_g$	0.00004	0.21(11)	0.033	0.035	0.31(2)	0.31(4)
$2_{\beta'} \rightarrow 2_g$	0.19	0.11(6)	1.3	0.065	1.2(1)	0.24
$2_{\beta'} \rightarrow 4_g$	<1.6[a]	2.7(14)	0.41	1.1	4.3(4)	1.4(2)
$0_{\beta'} \rightarrow 2_\beta$	29	40(16)				
$2_{\beta'} \rightarrow 0_\beta$	<1.2[a]	≤0.5	1.6	<1[b]	<0.3	
$2_{\beta'} \rightarrow 2_\beta$	11	9(5)	16	11		
$2_{\beta'} \rightarrow 4_\beta$		40(21)		21		
$2_{\beta'} \rightarrow 2_\gamma$	13		21	<2[b]	19(6)	
$2_{\beta'} \rightarrow 0_{\beta'}$	(110)[c]	184(100)	(100)[c]	(200)[c]		
			$10^3\rho^2(E0)$ [d]			
$0_{\beta'} \rightarrow 0_g$	1.2	1.2(8)	3.9		3.0(13)	
$2_{\beta'} \rightarrow 2_g$	1.6		3.4	>0.8		0.6(2)
$0_{\beta'} \rightarrow 0_\beta$	(42)[e]	21(9)	(153)[e]		32(15)[f]	
$2_{\beta'} \rightarrow 2_\beta$	42	(21)[e]	153	67		
$2_{\beta'} \rightarrow 2_\gamma$	17					
			$B(E1)$ (10^4 W.u.)			
$0_{\beta'} \rightarrow 1_1^-$		9(3)				
$2_{\beta'} \rightarrow 1_1^-$	2.4	5(2)		<5		0.64(8)
$2_{\beta'} \rightarrow 3_1^-$	2.0	6(3)	3.6	3		1.9(2)

[a] Deduced from γ spectra of Ref. [22].
[b] From Ref. [64, 65].
[c] Adopted rate (see text) to normalize relative rates for the $2_{\beta'}$ state.
[d] $\rho^2(E0)$ deduced using the electronic factors Ω from Ref. [57].
[e] Equal $\rho^2(E0)$ rates between β' and β bands were assumed to normalize relative rates for the $0_{\beta'}$ state.
[f] From Ref. [79] with the assigned uncertainty of 35%.

Although PPQ reproduces most of the experimental values quite well, significant differences are observed for the $2^+_\beta \rightarrow 2^+_g$, $2^+_\gamma \rightarrow 2^+_g$, and $0^+_{\beta'} \rightarrow 2^+_g$ transitions. The aforementioned 2^+_β and 2^+_γ states seem to remain "unmixed" in the PPQ calculations making the PPQ results similar to those of the correspondence interpretation where the $B(E2; 2^+_\beta \rightarrow 2^+_g)$ rate is *slow* at ≥ 1 W.u. and the $B(E2; 2^+_\gamma \rightarrow 2^+_g)$ rate is *transitional* at 30–50 W.u. These states appear to be correctly treated in the DPPQ model giving a good agreement with the data. It is important to extend the DPPQ calculations to the higher-lying levels.

TABLE V. Experimental and theoretical $B(E2)$ and $\rho^2(E0)$ rates for ^{150}Sm.

$I_i \rightarrow I_f$	Experimental[a]	PPQ[b]	DPPQ[c]
	$B(E2)$ (W.u.)		
$2_g \rightarrow 0_g$	57(1)	49	87
$2_\beta \rightarrow 0_\beta$	110(30)	29	70
$0_\beta \rightarrow 2_g$	54(5)	69	98
$2_\beta \rightarrow 0_g$	0.8(2)	0.61	1.6
$2_\beta \rightarrow 2_g$	65(15)	0.42	23
$2_\beta \rightarrow 4_g$	110(40)	19	21
$4_\gamma \rightarrow 2_\gamma$	$\sim$70[d]	57	
$2_\gamma \rightarrow 0_g$	2.0(4)	2.0	3.0
$2_\gamma \rightarrow 2_g$	9(2)	26	5.7
$2_\gamma \rightarrow 4_g$	5(2)	7.1	11
$4_\gamma \rightarrow 2_g$	$\sim$0.7[d]	0.5	1.9
$4_\gamma \rightarrow 4_g$	$\sim$14[d]	18	7.4
$2_\gamma \rightarrow 0_\beta$	19(6)	20	21
$2_\gamma \rightarrow 2_\beta$	100(60)	48	116
$2_{\beta'} \rightarrow 0_{\beta'}$	(110)		
$0_{\beta'} \rightarrow 2_g$	0.17	0.0002	
$0_{\beta'} \rightarrow 2_\beta$	29	36	
	$10^3\rho^2(E0)$[e]		
$0_\beta \rightarrow 0_g$	17(2)	22	78
$2_\beta \rightarrow 2_g$	90(35)	15	63
$0_{\beta'} \rightarrow 0_g$	1.2	0.32	
$2_{\beta'} \rightarrow 2_\beta$	1.6		
$0_{\beta'} \rightarrow 0_\beta$	42	26	
$2_{\beta'} \rightarrow 2_\gamma$	17		

[a] Data from Refs. [72, 78] and Table IV.
[b] Pairing-plus-quadrupole model [3].
[c] Dynamic pairing-plus-quadrupole model [6, 7].
[d] From systematics of the heavy Sm and Gd nuclei.
[e] $\rho^2(E0)$ deduced using the electronic factors Ω from Ref. [57].

V. SUMMARY AND CONCLUSIONS

A number of new transitions and levels have been identified in the low-spin β^- decay of ^{152}Pm$\rightarrow^{152}$Sm. A half-life of 15(6) ps and new branching ratios have been measured for the 0^+_3 state and the $B(E2)$ and $\rho^2(E0)$ rates have been deduced for the transitions deexciting the 0^+ and 2^+ members of the 0^+_3 band.

The new results confirm the transition rates calculated with the PPQ model [3] and thus support the interpretation of the β' band as the m band. Moreover, they give some weight to the controversial conclusion drawn by Kumar who questioned [3] the shape coexistence interpretation of the 0^+_3 band and, as a consequence, of the Sm-Gd region. Further theoretical studies of the β' bands are necessary. Yet the real issue here may not be the occurence of shape coexistence in ^{152}Sm but rather whether the $B(E2)$ and $E0$ transition rates, as well as the cross sections in the (p,t) and (t,p) reactions, directly depend on the large differences in shape, or alternatively whether they depend on the microscopic composition alone.

^{152}Sm and ^{114}Cd represent classical cases of shape coexistence, where the shape-coexistence interpretation has been recently challenged [26–28]. The results for both nuclei can be understood within the correspondence interpretation [29–31], here extended to include the correspondence pattern of $B(E2)$ rates. We have constructed the $B(E2)$ rate and level systematics in the transitional Sm-Gd nuclei and found it consistent with the correspondence interpretation up to and including the 0^+_3 band. Moreover, the patterns of transition rates were found largely independent on the "intruder" or "shape-coexistence" features of the bands.

The β and γ bands which bandheads evolve from the $N=2$ vibrational multiplets represent [1] two basic and distinctively different excitation modes. One may ask whether the bands which bandheads evolve from the $N=3$ or even higher-order multiplets are also associated with new and distinctively different excitation modes. A number of facts discussed here, such as the uncorrelated excitation energies for the β and β' bands in heavy Sm and Gd, the high selectivity of the β^- decay, and the closely anticorrelated high selectivity of the (p,t) reaction for ^{152}Sm, affirm that the β and β' states have different intrinsic structures. Yet the β, γ, and β' bands show not only distinctively different properties based on different intrinsic structures but also common features like smooth correlations of the relative excitation energies and of the transition rates. The β' band could thus represent a new mode of intrinsic excitation in par with the β and γ modes. (In the rotational limit the β' band would naturally represent a different intrinsic excitation [1]; the issue here is that β' appears to represent a *different mode of excitation already distinctive in the transitional nuclei.*) On the other hand, β', as the $N=3$ mode of excitation, could be more complex than the $N=2$ β and γ modes. This could explain the inability of the phenomenological models based on a severely truncated space to account for the band and the neccessity to invoke the intruder picture.

The intrinsic structure of the β' bands remains open

for interpretation. Kumar [2, 3] has called it the m band — "a new type of band," representing a strong mixing of prolate, spherical, and oblate shapes to a point where K is not a good quantum number and coupling between rotations and vibrations cannot be neglected [2]. Our suggested interpretation of the β' band as a new and distinctive mode of excitation appears somewhat different to the m band interpretation as a mixed structure. It would be of great interest to see more detailed and systematic calculations of the β' bands via the DPPQ and other microscopical models. Moreover, these calculations should include the higher-lying 0_4^+ and 0_5^+ states which may represent higher excitation modes of the β and β' bands, respectively, which could evolve from the 0^+ vibrational states with phonon numbers N=5 and N=4.

The results of this work call for a critical reanalysis of the Sm-Gd transitional region and the Cd nuclei using the microscopic models. From the view of theoretical interest, new experimental work is called upon to provide more precise data on the 0_3^+ and higher-lying bands. Particularly important are the heavy-ion Coulomb excitation studies of the kind done by Fahlander *et al.* [26] on ^{114}Cd. The case is particularly favorable as all nuclei of interest are stable. Moreover, a high-sensitivity study of the low-spin decay of ^{154}Tb is strongly needed.

Finally, the correspondence interpretation intended as a schematic representation of the smooth structural changes that occur in the transition from vibrational to rotational nuclei was found to be a convenient tool (a benchmark) to classify the experimental data and to uncover major departures from its simple patterns.

ACKNOWLEDGMENTS

Stimulating discussions with C. Fahlander, J. Kumpulainen, R. Julin, and J. Kantele are gratefully acknowledged. This work has been supported by the Swedish Natural Science Research Council.

[1] A. Bohr and B. R. Mottelson, *Nuclear Structure* (Benjamin, New York, 1975), Vol. 2.
[2] K. Kumar, Nucl. Phys. A **92**, 653 (1967).
[3] K. Kumar, Nucl. Phys. A **231**, 189 (1974).
[4] J. B. Gupta, K. Kumar, and J. H. Hamilton, Phys. Rev. C **16**, 427 (1977).
[5] K. Kumar and J. B. Gupta, Nucl. Phys. A **304**, 295 (1978).
[6] J. B. Gupta and K. Kumar, J. Phys. G **7**, 673 (1981).
[7] J. B. Gupta, Phys. Rev. C **28**, 1829 (1983).
[8] T. Kishimoto and T. Tamura, Nucl. Phys. A **270**, 317 (1976), and references therein.
[9] T. Tamura, K. Weeks, and T. Kishimoto, Phys. Rev. C **20**, 307 (1979).
[10] T. Tamura, K. Weeks, and T. Kishimoto, Nucl. Phys. A **347**, 359 (1980).
[11] O. Scholten, F. Iachello, and A. Arima, Ann. Phys. (N.Y.) **115**, 325 (1978), and references therein.
[12] P. Van Isacker, K. Heyde, M. Waroquier, and G. Wenes, Nucl. Phys. A **380**, 383 (1982).
[13] H. J. Daley and M. A. Nagarajan, Phys. Lett. **166B**, 379 (1986).
[14] S. Hinds, J. H. Bjerregaard, O. Hansen, and O. Nathan, Phys. Lett. **14**, 48 (1965).
[15] J. H. Bjerregaard, O. Hansen, O. Nathan, and S. Hinds, Nucl. Phys. **86**, 145 (1966).
[16] W. McLatchie, J. E. Kitching, and W. Darcey, Phys. Lett. **30B**, 529 (1969).
[17] P. Debenham and N. M. Hintz, Phys. Rev. Lett. **25**, 44 (1970).
[18] W. McLatchie, W. Darcey, and J. E. Kitching, Nucl. Phys. A **159**, 615 (1970).
[19] P. Debenham and N. M. Hintz, Nucl. Phys. A **195**, 385 (1972).
[20] L. L. Riedinger, N. R. Johnson, and J. H. Hamilton, Phys. Rev. **179**, 1214 (1969).
[21] L. L. Riedinger, N. R. Johnson, and J. H. Hamilton, Phys. Rev. C **2**, 2358 (1970).
[22] J. Barrette, M. Barette, A. Boutard, G. Lamoureux, S. Monaro, and S. Markiza, Can. J. Phys. **49**, 2462 (1971).
[23] N. Rud, H. L. Nielsen, and K. Wilsky, Nucl. Phys. A **167**, 401 (1971).
[24] N. Rud, G. T. Ewan, A. Christy, D. Ward, R. L. Graham, and J. S. Geiger, Nucl. Phys. A **191**, 545 (1972).
[25] A. Faessler, Nucl. Phys. A **396**, 291c (1983).
[26] C. Fahlander, A. Bäcklin, L. Hasselgren, A. Kavka, V. Mittal, L. E. Svensson, B. Varnestig, D. Cline, B. Kotlinski, H. Grein, E. Grosse, R. Kulessa, C. Michel, W. Spreng, H. J. Wollersheim, and J. Stachel, Nucl. Phys. A **485**, 327 (1988).
[27] H. Mach, M. Moszyński, R. F. Casten, R. L. Gill, D. S. Brenner, J. A. Winger, W. Krips, C. Wesselborg, M. Büsher, F. K. Wohn, A. Aprahamian, D. Alburger, A. Gelberg, and A. Piotrowski, Phys. Rev. Lett. **63**, 143 (1989).
[28] J. Kumpulainen, R. Julin, J. Kantele, A. Passoja, W. H. Trzaska, E. Verho, and J. Väärämäki, Z. Phys. A **335**, 109 (1990); also Phys. Rev. C **45**, 640 (1992).
[29] R. K. Sheline, Rev. Mod. Phys. **32**, 1 (1960).
[30] M. Sakai, Nucl. Phys. A **104**, 301 (1967).
[31] M. Sakai, Nucl. Data Tables A **8**, 323 (1970).
[32] M. Sakai, At. Data. Nucl. Data Tables **31**, 399 (1984).
[33] K. Kumar, in *The Electromagnetic Interaction in Nuclear Spectroscopy*, edited by W. D. Hamilton (North-Holland, New York, 1975), p. 55.
[34] G. Gneuss, U. Mosel, and W. Greiner, Phys. Lett. **31B**, 269 (1970).
[35] R. A. Meyer, R. D. Griffioen, J. G. Lefler, and W. B. Walters, Phys. Rev. C **14**, 2024 (1976).
[36] S. V. Jackson and R. A. Meyer, Phys. Rev. C **15**, 1806 (1977).
[37] K. Heyde, P. Van Isacker, M. Waroquier, G. Wenes, and M. Sambataro, Phys. Rev. C **25**, 3161 (1982).
[38] S. Borg, I. Bergström, G. B. Holm, B. Rydberg, L.-E. De Geer, G. Rudstam, B. Grapengiesser, E. Lund, and L. Westergaard, Nucl. Instrum. Methods **91**, 109 (1971).
[39] L. Jacobsson, B. Fogelberg, B. Ekström, and G. Rudstam, Nucl. Instrum. Methods Phys. Res. B **26**, 223

(1987).
[40] H. Mach, R. L. Gill, and M. Moszyński, Nucl. Instrum. Methods Phys. Res. A **280**, 49 (1989).
[41] M. Moszyński and H. Mach, Nucl. Instrum. Methods Phys. Res. A **277**, 407 (1989).
[42] H. Mach, F. K. Wohn, G. Molnár, K. Sistemich, John C. Hill, M. Moszyński, R. L. Gill, W. Krips, and D. S. Brenner, Nucl. Phys. A **523**, 197 (1991).
[43] H. Mach, M. Moszyński, and R. L. Gill (unpublished).
[44] M. Hellström, H. Mach, B. Fogelberg, D. Jerrestam, and L. Spanier, Phys. Rev. C **43**, 1462 (1991).
[45] I. Tago, Y. Kawase, and K. Okano, Z. Phys. A **335**, 477 (1990).
[46] T. Karlewski, N. Hildebrand, M. Brügger, N. Kaffrell, N. Trautmann, and G. Herrmann, Z. Phys. A **330**, 55 (1988).
[47] H. Mach, F. K. Wohn, M. Moszyński, R. L. Gill, and R. F. Casten, Phys. Rev. C **41**, 1141 (1990).
[48] H. Mach, W. Nazarewicz, D. Kusnezov, M. Moszyński, B. Fogelberg, M. Hellström, L. Spanier, R. L. Gill, R. F. Casten, and A. Wolf, Phys. Rev. C **41**, R2469 (1990).
[49] L. K. Peker, Nucl. Data Sheets **58**, 93 (1989).
[50] K. P. Artamonova, V. M. Vinogradov, E. P. Grigor'ev, A. V. Zolotavin, V. M. Makarov, and V. O. Sergeev, Izv. Akad. Nauk SSSR, Ser. Fiz. **43**, 935 (1975) [Bull. Acad. Sci. USSR, Phys. Ser. **43**, 31 (1975)].
[51] N. M. Stewart, E. Eid, M. S. S. El–Daghmah, and J. K. Jabber, Z. Phys. A **335**, 13 (1990).
[52] V. M. Kartashov, A. I. Oborovskii, and A. G. Troitskaya, Izv. Akad. Nauk SSSR, Ser. Fiz. **54**, 169 (1990) [Bull. Acad. Sci. USSR, Phys. Ser. **54**, 173 (1990)].
[53] G. Wirth, N. Kaffrell, K. Chayawattanangkur, G. Herrmann, and K. E. Seyb, Z. Phys. A **272**, 291 (1975).
[54] H. Yamamoto, K. Kawade, Y. Ikeda, and T. Katoh, J. Phys. Soc. Jpn. **43**, 8 (1977).
[55] W. R. Daniels and D. C. Hoffmann, Phys Rev. C **4**, 919 (1971).
[56] S. Raman, C. W. Nestor, Jr., and K. H. Bhatt, Phys. Rev. C **37**, 805 (1988).
[57] J. Kantele, Nucl. Instrum. Methods Phys. Res. A **271**, 625 (1988).
[58] R. F. Casten and D. D. Warner, Rev. Mod. Phys. **60**, 389 (1988).
[59] A. Saha, O. Scholten, D. C. J. M. Hageman, and H. T. Fortune, Phys. Lett. **85B**, 215 (1979).
[60] R. J. Ascuitto and B. Sorensen, Nucl. Phys. A **190**, 309 (1972).
[61] P. C. Sood, D. M. Headly, and R. K. Sheline, At. Data Nucl. Data Tables **47**, 89 (1991).
[62] R. C. Greenwood, C. W. Reich, H. A. Baader, H. R. Koch, D. Breitig, O. W. B. Schult, B. Fogelberg, A. Bäckin, W. Mampe, T. von Egidy, and K. Schreckenbach, Nucl. Phys. A **304**, 327 (1978).
[63] M. A. M. Shahabuddin, D. G. Burke, I. Nowikow, and J. Waddington, Nucl. Phys. A **340**, 109 (1980).
[64] R. A. Meyer, Phys. Rev. **170**, 1089 (1968).
[65] R. A. Meyer, Phys. Rev. **174**, 1478 (1968).
[66] D. C. Sousa, L. L. Riedinger, E. G. Funk, and J. W. Mihelich, Nucl. Phys. A **238**, 365 (1975).
[67] D. G. Fleming, C. Günther, G. B. Hagemann, and B. Herskind, Phys. Rev. Lett. **27**, 1235 (1971).
[68] D. G. Fleming, C. Günther, G. Hagemann, B. Herskind, and P. O. Tjom, Phys. Rev. C **8**, 806 (1973).
[69] Ts. Vylov, I. I. Gromova, V. V. Kuznetsov, V. G. Nedovesov, V. I. Fominykh, Yu. V. Kholnov, and G. E. Shchukin, Bull. Acad. Sci. USSR, Phys. Ser. **36**, 649 (1972).
[70] R. G. Helmer, Nucl. Data Sheets **52**, 1 (1987).
[71] L. K. Peker, Nucl. Data Sheets **59**, 393 (1990).
[72] E. der Mateosian, Nucl. Data Sheets **48**, 345 (1986).
[73] R. G. Helmer, Nucl. Data Sheets **49**, 383 (1986).
[74] M. A. Lee, Nucl. Data Sheets **56**, 199 (1989).
[75] B. Varnestig, Ph.D. thesis, University of Uppsala, 1987.
[76] F. K. McGowan and W. T. Milner, Phys. Rev. C **23**, 1926 (1981).
[77] J. Lange, K. Kumar, and J. H. Hamilton, Rev. Mod. Phys. **54**, 119 (1982).
[78] R. K. Smither, Phys. Rev. **150**, 964 (1966).
[79] F. Hoyler, K. Schreckenbach, H. G. Börner, and G. Colvin, in *Capture Gamma-Ray Spectroscopy and Related Topics–1984*, edited by S. Raman, AIP Conference Proceedings No. 125 (American Institute of Physics, New York, 1985), p. 410.